J|A|C|S
ARTICLES
Published on Web 03/22/2007

Molecular Mimicry Enables Competitive Recruitment by a Natively Disordered Protein

Daniel A. Bonsor,[†] Irina Grishkovskaya,[†] Eleanor J. Dodson,[‡] and Colin Kleanthous*,[†]

Contribution from the Department of Biology, University of York, Heslington, York, YO10 5YW, United Kingdom and York Structural Biology Laboratory, Department of Chemistry, University of York, Heslington, York, YO10 5DD, United Kingdom

Received January 9, 2007; E-mail: ck11@york.ac.uk

Abstract: We report the crystal structure of the *Escherichia coli* TolB-Pal complex, a protein−protein complex involved in maintaining the integrity of the outer membrane (OM) in all Gram-negative bacteria that is parasitized by colicins (protein antibiotics) to expedite their entry into cells. Nuclease colicins competitively recruit TolB using their natively disordered regions (NDRs) to disrupt its complex with Pal, which is thought to trigger translocation of the toxin across a locally destabilized OM. The structure shows induced-fit binding of peptidoglycan-associated lipoprotein (Pal) to the β-propeller domain of TolB causing the N-terminus of one of its α-helices to unwind and several residues to undergo substantial changes in conformation. The resulting interactions with TolB are known to be essential for the stability of the complex and the bacterial OM. Structural comparisons with a TolB-colicin NDR complex reveal that colicins bind at the Pal site, mimicking rearranged Pal residues while simultaneously appearing to block induced-fit changes in TolB. The study therefore explains how colicins recruit TolB in the bacterial periplasm and highlights a novel binding mechanism for a natively disordered protein.

Introduction

The outer membrane (OM) of *Escherichia coli* is a formidable but selective barrier that shields the organism from large antibiotics and bile salts while allowing the passive diffusion of small nutrients and metabolites through protein pores.[1−3] Biogenesis of the OM and maintenance of its integrity are therefore vital for cell viability of all Gram-negative bacteria and as such represents a key target for the development of novel antimicrobials. The mechanisms underlying these processes are, however, poorly understood. One in particular that has been well studied for many years yet remains uncharacterized at the molecular level is the Tol-Pal system, a supramolecular assembly of proteins that bridges the two membranes and is required for stability of the OM.[4,5]

The Tol-Pal system is comprised of five core proteins: TolA, TolQ, and TolR are inner membrane (IM) proteins that associate through their transmembrane helices, while TolB and Pal form a complex at the OM as well as interacting with the periplasm-spanning TolA.[4,5] Pal (13 kDa) is inserted into the inner leaflet of the OM through a lipoyl tether and associates with peptidoglycan (PG), providing important noncovalent, stabilizing cross bridges between the OM and the PG layer.[6−8] TolB (44 kDa) acts as a network hub interacting with both TolA and Pal[9,10] but also with a number of other outer membrane proteins such as Lpp and OmpA.[7] Deletion or mutation of any of the five core proteins within the Tol-Pal assembly leads to increased bacterial susceptibility to toxic compounds such as SDS and antibiotics such as rifampicin, both of which are normally excluded by the OM.[11] This is accompanied by extensive 'blebbing' of the membrane and leakage of periplasmic contents.[12] Whatever the precise physiological role of the Tol-Pal system it is clear that it requires an energy source since the protein−protein interactions between TolA and TolB/Pal are coupled to the proton motive force (PMF) across the IM.[13,14] Consistent with this requirement, TolQ and TolR are homologues of other PMF-dependent systems in bacteria including MotA and MotB, which drive the flagellar motor, and ExbB and ExbD, which energize OM nutrient receptors for active transport via the IM protein TonB.[15]

[†] Department of Biology.
[‡] Department of Chemistry.

(1) Nikaido, H. *Microbiol. Mol. Biol. Rev.* **2003**, *67*, 593−656.
(2) Bos, M. P.; Tommassen, J. *Curr. Opin. Microbiol.* **2004**, *7*, 610−616.
(3) Ruiz, N.; Kahne, D.; Silhavy, T. J. *Nat. Rev. Microbiol.* **2006**, *4*, 57−66.
(4) Lloubès, R.; Cascales, E.; Walburger, A.; Bouveret, E.; Lazdunski, C.; Bernadac, A.; Journet, L. *Res. Microbiol.* **2001**, *152*, 523−529.
(5) Lazzaroni, J. C.; Dubuisson, J. F.; Vianney, A. *Biochimie* **2002**, *84*, 391−397.
(6) Gennity, J. M.; Inouye, M. *J. Biol. Chem.* **1991**, *266*, 16458−16464.
(7) Clavel, T.; Germon, P.; Vianney, A.; Portalier, R.; Lazzaroni, J. C. *Mol. Microbiol.* **1998**, *29*, 359−367.
(8) Cascales, E.; Lloubès, R. *Mol. Microbiol.* **2004**, *51*, 873−885.
(9) Bouveret, E.; Derouiche, R.; Rigal, A.; Lloubès, R.; Lazdunski, C.; Bénédetti, H. *J. Biol. Chem.* **1995**, *270*, 11071−11077.
(10) Bouveret, E.; Bénédetti, H.; Rigal, A.; Loret, E.; Lazdunski, C. *J. Bacteriol.* **1999**, *181*, 6306−6311.
(11) Webster, R. E. *Mol. Microbiol.* **1991**, *5*, 1005−1011.
(12) Bernadac, A.; Gavioli, M.; Lazzaroni, J. C.; Raina, S.; Lloubès, R. *J. Bacteriol.* **1998**, *180*, 4872−4878.
(13) Cascales, E.; Gavioli, M.; Sturgis, J. N.; Lloubès, R. *Mol. Microbiol.* **2000**, *38*, 904−915.
(14) Germon, P.; Ray, M. C.; Vianney, A.; Lazzaroni, J. C. *J. Bacteriol.* **2001**, *183*, 4110−4114.

10.1021/ja070153n CCC: $37.00

When faced with environmental stress bacteria often release bacteriocins, protein toxins that selectively kill neighboring microbes.[16−18] These potent antibiotics are able to bind cell surface receptors and translocate into the susceptible bacterium through a series of protein−protein interactions with membrane-bound and periplasmic proteins. Tol-Pal is one of the major routes used by bacteriocins and filamentous bacteriophages alike to reach the periplasm, the other being the TonB/ExbB/ExbD complex.[18,19] Most microorganisms produce some type of bacteriocin, including *E. coli*, *Salmonella typhimurium*, *Pseudomonas aeruginosa*, *Listeria monocytogenes*, and *Yersinia pestis*, where they play important roles in bacterial competition, virulence, adaptation, and diversification.[20−22] Bacteriocins that target *E. coli* are known as colicins, their synthesis and release from a producing cell induced via the SOS stress response.[18] It has been estimated that one-third of all *Enterobacteriacea* are colicinogenic with >20 different plasmid-encoded colicins thus far identified.

Colicins are multidomain proteins composed of a central receptor-binding domain flanked by an N-terminal domain involved in OM translocation and a C-terminal cytotoxic domain that is translocated either to the periplasm, where the toxin can depolarize the IM or degrade peptidoglycan precursors, or the cytoplasm, where it degrades nucleic acid.[18,19] E group colicins E2-E9 utilize the vitamin B_{12} receptor, BtuB, as their primary receptor and translocate one of three structurally distinct nucleases to the cytoplasm (tRNase, rRNase, DNase), emphasizing that import is structure independent. BtuB binding localizes the toxin to the cell surface from where it recruits the porin OmpF using an N-terminal 83 amino acid, natively disordered region (NDR) that is part of its translocation domain.[23−27] The lumen of an OmpF subunit is thought to be the route taken by the NDR to the periplasm where it next recruits TolB, an association that appears to trigger translocation into the cell.[25,26,28] We demonstrated recently that nuclease colicins competitively recruit TolB from its complex with Pal, the colicin and Pal having approximately equivalent binding affinities for TolB ($K_d \approx 90$ nM) when TolB is bound with divalent cations, and determined the crystal structure of TolB bound to the 16-residue TolB-binding epitope of colicin E9 (ColE9).[29]

In the present work we elucidated the structure of the TolB-Pal complex and explored the thermodynamics of association to investigate the physicochemical properties of the complex. By comparison to our previous work on TolB and its association with the ColE9 NDR we discovered how this class of bacteriocin is able to use its NDR to disrupt the TolB-Pal complex in order to expedite toxin entry to the periplasm.

Experimental Methods

Protein Expression and Purification. The plasmids encoding TolB and Pal with a C-terminal His-6 tail were expressed and purified as described previously.[29] The concentrations of purified TolB and Pal were determined spectrophotometrically using the molar extinction coefficients, ϵ_{280}, of 57 870 and 11 920 M^{-1} cm^{-1}, respectively.

Isothermal Titration Calorimetry (ITC) Measurements. ITC experiments were carried out on a VP-ITC in 50 mM buffer, 50 mM NaCl, 5 mM EDTA, pH 7.5 at 20 °C, where buffer was sodium phosphate, Hepes, MES, BES, or TES. TolB was normally in the sample cell and Pal in the injection syringe at concentrations of 31.7 and 281 μM, respectively. The titration consisted of 35 injections of 2−8 μL with an interval of 240 s between injections. Heats of dilutions were measured and subtracted from each data set. All samples were degassed prior to titration. Data were analyzed using Origin 7.0 software.

Crystallization, Data Collection, Structure Determination, and Refinement. A 1:1 TolB-Pal complex was prepared by mixing the two components together, with Pal in slight excess and then purified on a Superdex S75 26/60 column. The purified complex was dialyzed against 50 mM Tris, pH 7.5, concentrated to 44 mg mL^{-1} and dialyzed against 0.1 M sodium acetate, pH 4.6. Crystals were obtained by the hanging drop method, where 1 μL of complex was mixed with 1 μL of the reservoir solution (20% polyethylene glycol 2000 monomethyl ether, 0.2 M ammonium sulfate, and 0.1 M sodium acetate pH 4.6). Crystals grew within 2−3 days and were flash cooled in mother liquid containing 20% glycerol. A data set was collected at the European Synchrotron Radiation Facility beamline ID14-2 at 100 K and reduced with MOSFLM and SCALA of the CCP4 suite of programs.[30] The structure was solved by molecular replacement through the program MOLREP using the atomic coordinates of TolB and Pal as search models (PDB, 1C5K,[35] and 1OAP, respectively). The structure was refined using REFMAC,[31] and rebuilding was done using Coot.[32] Coordinates have been deposited in the protein data bank (PDB, 2HQS). All figures were produced with either PyMol[33] or CCP4mg.[34]

Results

Overview of the TolB-Pal Complex. TolB and the soluble domain of Pal were complexed and crystallized as described in the Experimental Methods and the structure solved by molecular replacement. Data refinement statistics are shown in Table 1. Four complexes were found in the asymmetric unit with no significant differences between them; chain A and H (TolB and Pal, respectively) were used for detailed analysis. The TolB-Pal complex is shown in Figure 1a with typical electron density

(15) Cascales, E.; Lloubès, R.; Sturgis, J. N. *Mol. Microbiol.* **2001**, *42*, 795−807.
(16) *Bacteriocins, Microcins and Lantibiotics*; James, R., Lazdunski, C., Pattus, F., Eds.; NATO ASI Series H; Springer: Heidelberg, 1992.
(17) Lazdunski, C. J.; Bouveret, E.; Rigal, A.; Journet, L.; Lloubès, R.; Bénédetti, H. *J. Bacteriol.* **1998**, *180*, 4993−5002.
(18) James, R.; Penfold, C. N.; Moore, G. R.; Kleanthous, C. *Biochemie* **2002**, *84*, 381−389.
(19) Braun, V.; Patzer, S. I.; Hantke, K. *Biochemie* **2002**, *84*, 365−380.
(20) Czárán, T. L.; Hoekstra, R. F.; Pagie, L. *Proc. Natl. Acad. Sci. U.S.A.* **2002**, *99*, 786−790.
(21) Kerr, B.; Riley, M. A.; Feldman, M. W.; Bohannan, B. J. M. *Nature* **2002**, *418*, 171−174.
(22) Kirkup, B. C.; Riley, M. A. *Nature* **2004**, *428*, 412−414.
(23) Soelaiman, S.; Jakes, K.; Wu, N.; Li, C. M.; Shoham, M. *Mol. Cell.* **2001**, *8*, 1053−1062.
(24) Collins, E. S.; Whittaker, S. B. M.; Tozawa, K.; MacDonald, C.; Boetzel, R.; Penfold, C. N.; Reilly, A.; Clayden, N.; Osborne, M. J.; Kleanthous, C.; James, R.; Moore, G. R. *J. Mol. Biol.* **2002**, *318*, 787−904.
(25) Kurisu, G.; Zakharov, S. D.; Zhalnina, M. V.; Bano, S.; Eroukova, V. Y.; Rokitskaya, T. I.; Antonenkom, Y. N.; Wiener, M. C.; Cramer, W. A. *Nat. Struct. Biol.* **2003**, *10*, 948−954.
(26) Housden, N. G.; Loftus, S.; Moore, G. R.; James, R.; Kleanthous, C. *Proc. Natl. Acad. Sci. U.S.A.* **2005**, *102*, 13849−13854.
(27) Tozawa, K.; Macdonald, C. J.; Penfold, C. N.; James, R.; Kleanthous, C.; Clayden, N. J.; Moore, G. R. *Biochemistry* **2005**, *44*, 11496−11507.
(28) Zakharov, S. D.; Eroukova, V. Y.; Rokitskaya, T. I.; Zhalnina, M. V.; Sharma, O.; Loll, P. J.; Zgurskaya, H. I.; Antonenko, Y. N.; Cramer, W. A. *Biophys. J.* **2004**, *87*, 3901−3911.
(29) Loftus, S. R.; Walker, D.; Maté, M. J.; Bonsor, D. A.; James, R.; Moore, G. R.; Kleanthous, C. *Proc. Natl. Acad. Sci. U.S.A.* **2006**, *103*, 12353−12358.
(30) Collaborative Computational Project, Number 4. *Acta Crystallogr., D: Biol. Crystallogr.* **1994**, *50*, 760−763.
(31) Murshudov, G. N.; Vagin, A. A.; Dodson, E. J. *Acta Crystallogr., D: Biol. Crystallogr.* **1997**, *53*, 240−255.
(32) Emsley, P.; Cowtan, K. *Acta Crystallogr., D: Biol. Crystallogr.* **2004**, *60*, 2126−2132.
(33) DeLano, W. L. *The PyMOL User's Manual*; DeLano Scientific: San Carlos, CA, 2002.
(34) Potterton, E.; McNicholas, S.; Krissinel, E.; Cowtan, K.; Noble, M. *Acta Crystallogr., D: Biol. Crystallogr.* **2002**, *58*, 1955−1957.

Table 1. Summary of Crystallographic Analysis

	TolB-Pal complex
data collection	
space group	*P*1
cell dimensions	
a, *b*, *c* (Å)	74.85, 89.05, 91.05
α, *β*, *γ* (deg)	87.15, 89.62, 68.81
resolution (Å)[a]	40−1.5 (1.58−1.5)
R_{merge}[a,b]	4.4 (26.6)
$I/\sigma I$[a]	8.7 (1.9)
completeness (%)[a]	95.4 (94.1)
redundancy[a]	2.0 (2.0)
refinement	
resolution (Å)	40−1.5 Å
no. of reflns	317 580
R_{work}/R_{free}	18.0/21.3
B factors (Å^2)	
TolB	13.22
Pal	20.75
water	32.46
rms deviations[c]	
bond lengths (Å)	0.009
bond angles (deg)	1.23

[a] Limits and values for the outer resolution bin are given in parentheses. [b] $R_{merge} = \Sigma\Sigma|I_{i,j} - \langle I_j \rangle|/\Sigma\Sigma I_{i,j}$. [c] Root-mean-square deviation given from ideal values.

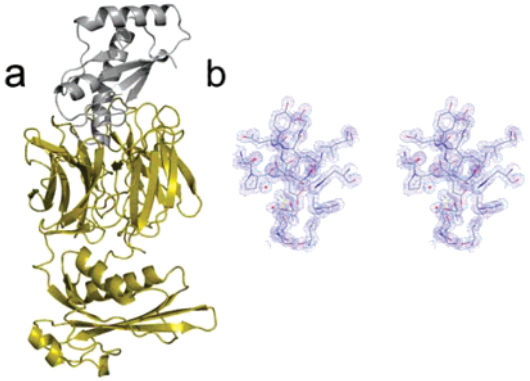

Figure 1. (a) Ribbon representation of the TolB-Pal complex. Pal (gray) binds on the TolB (yellow) *β*-propeller. (b) Stereorepresentation of the $2F_O - F_C$ σ_A-weighted electron density map contoured at 1.5 σ showing interface residues.

from the 1.5 Å structure shown in Figure 1b. TolB is comprised of an N-terminal mixed α/*β* domain and a C-terminal six-bladed *β*-propeller domain. Strands connecting the propeller blades form a bowl at the bottom of which is a channel that traverses the domain. In previous TolB structures one or more metal ions were located within this channel, although none were observed in the TolB-Pal complex.[29,35] Pal binds within the bowl of the *β*-propeller domain blocking the central channel and contacting all of the connecting loops and several of the *β*-strands of the blades. Pal is comprised of a four-stranded mixed *β*-sheet and four α-helices, the longest of which (helix III) is bent and forms one of the principle contacts with TolB (Site 1; residues 110−130) and the other comprising a short *β*-strand, part of a short helix and a linker sequence (Site 2; residues 144−163) (Figure 2a,b). Site 1 overlaps the site of TolB binding identified by Cascales and Lloubes using deletion analysis and cross-linking experiments (residues 94−121).[8] The involvement of Site 2 has not previously been described. Thirteen intermolecular hydrogen bonds stabilize the complex, one via a bridging water molecule;

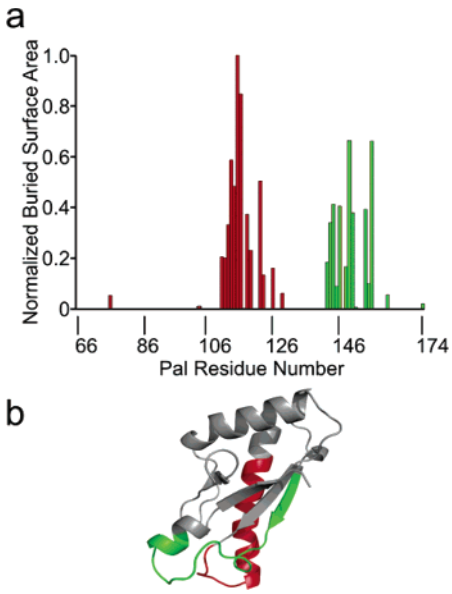

Figure 2. (a) Normalized buried surface area of Pal residues reveals two discontinuous TolB binding epitopes. Site 1, encompassing helix III, is shown in red with the neighboring loop and strand (Site 2) shown in green. (b) Structure of bound Pal with Sites 1 and 2 colored as in a.

Table 2. Interprotein Hydrogen Bonds in the TolB-Pal Complex

Pal	TolB	distance (Å)
N Gly113	NE2 Gln357	2.90
O Gly113	OE1 Gln357	2.84
OG1 Thr114	OE2 Glu293	2.67
OG1 Thr114	NE2 Gln336	2.94
OE1 Glu116	OG Ser205	2.66
OE1 Glu116	N Ala249	2.92
OE2 Glu116	NE2 His246	2.79
OH Tyr117	OD2 Asp308	2.58
OE2 Glu123	OG Ser264	2.53
ND2 Asn127	NH2 Arg245	2.97
NZ Lys150	OE1 Glu379	2.74
NZ Lys152	NE2 Gln201	2.80
NE2 His158	O Gly397	2.71

seven originate from just three Pal Site 1 residues (Gly113, Thr114, and Glu116), the remainder emanate from Pal Tyr117, Glu123, Asn127, Lys150, Lys152, and His158 (see Table 2 for complete list of hydrogen bonds). The calculated shape complementarity index, S_c,[36] for the TolB-Pal complex is 0.70, where 0 indicates no complementarity and 1 indicates perfect complementarity. The value for TolB-Pal is equivalent to that of high-affinity protein−protein complexes such as the colicin E9 DNase-Im9 and the barnase-barstar,[37,38] emphasizing the interface has a high degree of shape complementarity.

Conformational Changes Accompany Formation of the TolB-Pal Complex. The TolB-Pal complex buries 2600 Å^2 solvent-accessible surface area, which is much greater than the average buried surface area (∼1600 Å^2) for a protein−protein complex.[39,40] Complexes that bury such large surface areas often experience conformational changes,[39,40] which is also the case

(35) Carr, S.; Penfold, C. N.; Bamford, V.; James, R.; Hemmings, A. M. *Structure* **1999**, *8*, 57−66.
(36) Lawrence, M. C.; Colman, P. M. *J. Mol. Biol.* **1993**, *234*, 946−950.
(37) Buckle, A. M.; Schreiber, G.; Fersht, A. R. *Biochemistry* **1994**, *33*, 8878−8889.
(38) Kühlmann, U. C.; Pommer, A. J.; Moore, G. R.; James, R.; Kleanthous, C. *J. Mol. Biol.* **2000**, *301*, 1163−1178.
(39) Lo Conte, L.; Chothia, C.; Janin J. *J. Mol. Biol.* **1999**, *285*, 2177−2198.
(40) Janin, J. In *Protein-Protein Recognition*; Kleanthous, C., Ed.; Frontiers in Molecular Biology 31; Oxford University Press: New York, 2000; pp 1−59.

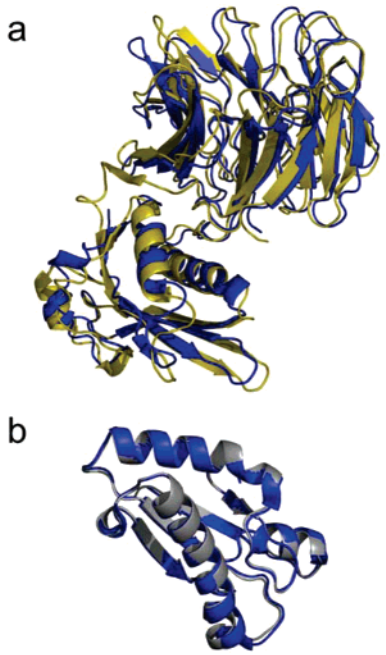

Figure 3. Structural superposition of (a) TolB in free (blue) and complexed (yellow) states and (b) Pal in the free (blue) and complexed (gray) states. Note the appearance of a new segment of antiparallel β-sheet at the domain−domain interface of TolB that forms as a result of complex formation with Pal. Changes in Pal are restricted to the N-terminus of helix III (bottom of the figure).

for the TolB-Pal complex. Binding occurs through an induced-fit mechanism in which both proteins undergo conformational changes. The root-mean-square deviation of the C_α atoms of the complex compared to unbound TolB and Pal are 1.5 Å and 0.4, respectively, demonstrating that the most significant changes occur in TolB. Importantly, Pal binding to TolB results in conformational changes being transmitted to its N-terminal α/β domain through the movement of loops and β-strands within the C-terminal propeller domain (Figure 3a). Surface-exposed loops distal to the N-terminal domain move only marginally (<1.5 Å), while three loops (with connecting β-strands) proximal to the domain move toward Pal by as much 5 Å, analogous to a 'venus fly trap' closing on its prey (Figure 3a). These movements result in changes to the adjoining domain−domain hinge region and creation of a two-stranded antiparallel β-sheet involving a strand from the β-propeller domain and the processed N-terminal end of TolB (residues 24−34), which has hitherto not been resolved in previous structures of TolB. Formation of this new hinge causes a global rearrangement of the N-terminal domain of TolB. The physiological consequences of these long-range conformational changes are unclear at present, although we note that TolA is reported to bind the N-terminal α/β domain of TolB[41] and TolB interactions with the outer membrane proteins OmpA and Lpp are dependent on its association with Pal.[7] Hence, it is likely that the conformational changes induced by Pal influences the ability of TolB to associate with other proteins in the OM and periplasm.

Pal also undergoes structural rearrangements, but these are localized to the N-terminus of helix III at Site 1 (Figure 3b) and are driven by clashes with two immobile TolB residues, Gln338 and Glu293 (Figure 4). The side chain of Pal Thr114

(41) Walburger, A.; Lazsunski, C.; Corda, Y. *Mol. Microbiol.* **2002**, *44*, 695−708.

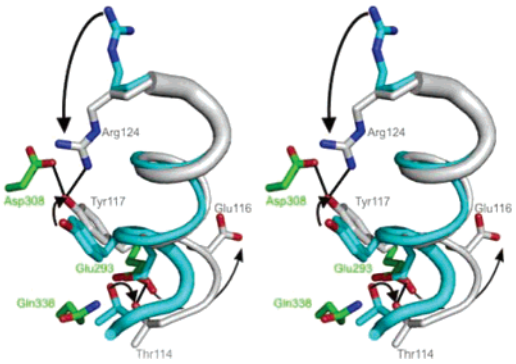

Figure 4. Stereofigure showing TolB-induced unwinding of Pal helix III. Several Pal residues reorient (black arrows), their new positions optimal for hydrogen bonding to TolB (green residues). Unbound Pal helix III is shown in cyan and TolB-bound Pal in gray. Hydrogen bonds are shown as black lines. Some residues (Glu116 and Arg124) rotate by as much as 180°.

forms the N-cap to Pal helix III in its unbound form but is forced to move 2.5 Å due to a clash with TolB Gln338, breaking the capping hydrogen bond to the main-chain atom of Pal Tyr117. The new position of Pal Thr114 is stabilized by a hydrogen bond with TolB Glu293, which itself engages in a severe steric and electrostatic clash with Pal Glu116, the side chain of which has to rotate by ~180° to avoid the clash and allowing it to engage in a critical hydrogen-bond network with TolB (see below). The consequence of these rearrangements is to disrupt two hydrogen bonds at the N-terminus of Pal helix III, causing it to unwind by 1.9 Å. Other side chains that reorient include Tyr117, which moves by 4.7 Å to a position stabilized by TolB Asp308 and Pal Arg124, the latter rotating by ~180° to meet it (Figure 4).

Comparison of Colicin NDR and Pal Binding to TolB. We demonstrated recently that a 16-residue epitope in the bacteriocin ColE9 NDR (residues 32−47) is sufficient to competitively recruit TolB from its complex with Pal, with cross-linking and mutational data suggestive of substantial overlap between the colicin and Pal binding sites on TolB.[29] We also solved the structure of the TolB-ColE9 NDR complex that provided the first structural information on how colicins bind periplasmic translocation portal proteins but did not explain the molecular mechanism of competitive recruitment. Through structural comparison of the TolB-ColE9 NDR and TolB-Pal complexes this issue can now be resolved.

Figure 5a shows a structural superposition of the TolB-Pal (present work) and TolB-ColE9 NDR complexes, which proves that the colicin NDR binds at the Pal site on TolB, the toxin adopting a fold distinct to that of Pal. Almost twice as much accessible surface area is buried in the TolB-Pal complex compared to the TolB-ColE9 NDR complex (2600 versus 1400 Å^2). The majority of the buried surface in the colicin complex coincides with that of Pal but not all; the colicin NDR makes additional contact with TolB (indicated in Figure 5b) through more efficient burial of side chains, resulting in the TolB-ColE9 NDR complex having a higher complementarity index (S_c = 0.78) than the TolB-Pal complex. The greater complementarity of the TolB-ColE9 NDR complex reflects the fact that the unfolded colicin is molded to fit the TolB surface in contrast to Pal, a globular protein that has to be distorted in order to bind. TolB and Pal bury 44 and 27 amino acids, respectively, in their complex, with roughly one-half the surface corresponding to Site 1 and the other half to Site 2 (Figure 5c). In contrast to the

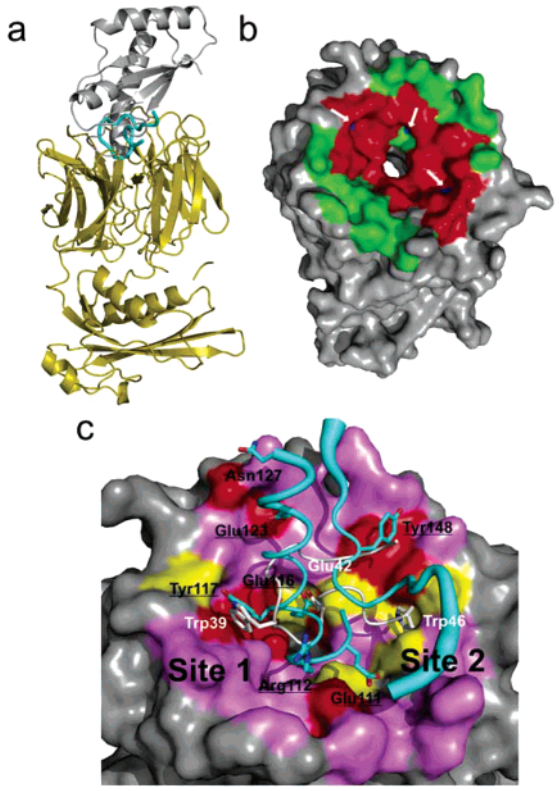

Figure 5. Superposition of the TolB-Pal (present work) and TolB-ColE9 NDR complexes. (a) Structural overlay of the two complexes showing how the ColE9 NDR (cyan) binds at the Pal (gray) site on the TolB (yellow) β-propeller. (b) Comparison of the accessible surface area buried on the TolB β-propeller by Pal (green) and the ColE9 NDR (blue, and highlighted with white arrows). Regions common to both complexes are colored red. (c) TolB surface colored according to sequence conservation (red, conserved; yellow, conservatively substituted; purple, variable) and showing ribbon depictions of Pal structural elements (cyan) and the ColE9 NDR (gray) bound to TolB. Pal residues are labeled black (underlines denote conserved amino acids), and ColE9 NDR residues are labeled white. The figure highlights how conserved Pal residues dock against conserved regions on TolB at Sites 1 and 2. The ColE9 NDR mimics Site 1 interactions while simultaneously occupying a binding pocket in Site 2 that is specific to the unbound state of TolB. This pocket becomes inaccessible when Pal binds due to conformational changes induced in TolB β-propeller loops.

13 intermolecular hydrogen bonds formed at the TolB-Pal interface, the ColE9 complex with TolB is stabilized by only five intermolecular hydrogen bonds; the majority of the colicins' hydrogen bonds are intramolecular, which provides stability to the bound conformation.

Although ubiquitous in Gram-negative organisms, TolB and Pal are poorly conserved proteins; for example, among 20 γ-proteobacteria sequences only ~13% and 19% of TolB and Pal residues, respectively, are identical. While the degree of sequence identity is doubled for the interface surfaces of each protein (25% and 44%, respectively) there remains a high proportion of sequence variability. Figure 5c shows the sequence conservation of the TolB binding surface and compares the binding conformations of Pal and ColE9 NDR. This depiction highlights a number of key points. First, conserved Pal side chains are recognized by conserved TolB residues across Site 1 and Site 2. These include van der Waals contacts between TolB Leu377 and the alkyl chains of Pal Glu111 and Arg112 and two hydrophobic TolB pockets that contact the phenyl rings of Pal Tyr 117 and Tyr148. Conserved polar and charged interactions include hydrogen bonds between Pal Glu123 and TolB Ser264 and between the hydroxyl of Pal Tyr117 and Asp308 and a hydrogen-bond network centered on Pal Glu116 involving TolB Ser205, His246, and Thr292 and two buried water molecules (Figure 6a).

Second, the ColE9 NDR is a molecular mimic of Pal helix III residues that have undergone conformational rearrangement as a result of binding to TolB. The distorted hairpin-fold adopted by ColE9 residues 35−43 allows it to occupy the same space within the TolB β-propeller bowl as the N-terminal two turns of Pal helix III. This positions Glu42 and Trp39 of the colicin so they mimic interactions made by helix III residues Glu116 and Tyr117, respectively, at Site 1 (Figure 6c). ColE9 Glu42 sits in the same deeply buried position as Pal Glu116 and engages in the same hydrogen-bond network with TolB (Figures 5c and 6), while ColE9 Trp39 docks onto the same hydrophobic pocket as Pal Tyr117 using its indole nitrogen to hydrogen bond TolB Asp308 as does the hydroxyl of Tyr117 (Figure 6b,c). Previous work has shown that mutation of TolB His246 to alanine abolishes both colicin and Pal binding in vitro and compromises TolB function in vivo, while mutation of ColE9 Trp39 or Glu42 abolishes TolB binding and colicin activity, indicating that these hydrogen-bond networks are critical to OM stability as well as colicin entry.[29,42]

Third, Trp46 of the ColE9 NDR, the mutation of which also abolishes TolB binding,[42] forms a unique contact with TolB for which no equivalent exists in the Pal complex. The indole side chain of Trp46 is buried deep within a pocket in Site 2 on the TolB surface that is not utilized by Pal (Figure 5c). Closer inspection of this region in the three available crystal structures of TolB (TolB, TolB-ColE9 NDR, TolB-Pal) shows that the pocket becomes constricted in the TolB-Pal complex due to the conformational changes induced by Pal, so that a large aromatic residue is no longer able to fit. In contrast, the colicin NDR does not induce any conformational changes in TolB, leaving the pocket open and accessible to Trp46. We speculate that a feature of the mechanism by which the NDR of ColE9 competitively recruits TolB is to occupy the Site 2 hydrophobic pocket and so block the ability of Pal to induce conformational changes in TolB. Consistent with this idea, preliminary experiments have shown that inclusion of 1 mM L-tryptophan in ITC experiments reduced the affinity of the TolB-Pal complex by ~6-fold (and 10 mM by 30-fold), in contrast to the equivalent concentration of L-alanine which had a negligible effect on binding (data not shown).

Thermodynamics of the TolB-Pal Association. The equilibrium dissociation constant for the TolB-Pal complex as determined by ITC is 27 nM at pH 7.5 and 20 °C in buffer containing 50 mM NaCl, with complex formation enthalpically and entropically favored.[29] In the present work, we found that the enthalpy of binding is strongly buffer dependent, suggestive of proton transfer being coupled to TolB-Pal complex formation, which is in contrast to ColE9 NDR binding to TolB where no such dependency exists. We therefore used ITC to investigate Pal binding TolB using buffers with different heats of ionization. The apparent enthalpy of binding, $\Delta H_{\text{apparent}}$, is the sum of the actual enthalpy of binding, $\Delta H_{\text{binding}}$, and the ionization enthalpy of buffer caused by proton exchange, $\Delta H_{\text{ionization}}$. Hence, the

(42) Hands, S. L.; Holland, L. E.; Vankemmelbeke, M.; Fraser, L.; MacDonald, C. J.; Moore, G. R.; James, R.; Penfold, C. N. *J. Bacteriol*. **2005**, *187*, 6733−6741.

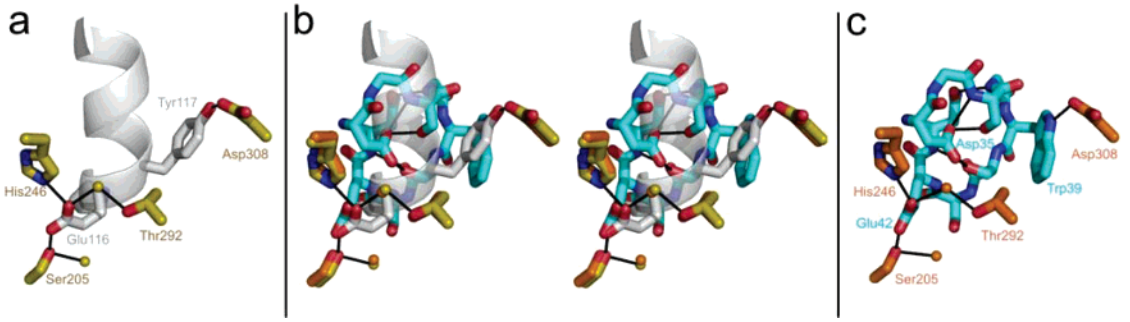

Figure 6. Competitive recruitment of TolB by the ColE9 NDR involves molecular mimicry of Pal Site 1 interactions. (a) Hydrogen-bond interactions of Pal helix III residues (gray) with TolB residues (green) formed as a result of the deformation to helix III (see Figure 4). (b) Stereoview showing a structural superposition of TolB-Pal and TolB-ColE9 NDR complexes highlighting the direct mimicry of Pal residues by the colicin. (c) Hydrogen-bond interactions of the ColE9 NDR (cyan) with TolB residues (orange).

actual enthalpy can be obtained by measuring binding using buffers with different heats of ionization and extrapolating back using the following relationship[43]

$$\Delta H_{\text{apparent}} = \Delta H_{\text{binding}} + N_{\text{H+}}\Delta H_{\text{ionization}} \qquad (1)$$

where N_{H+} is the number of protons that are released ($N_{H+} > 0$) or taken up ($N_{H+} < 0$) upon complexation. The five buffers employed had $\Delta H_{\text{ionization}}$ ranging from 1.46 to 7.86 kcal mol^{-1}. Figure 7a shows a typical ITC binding isotherm and Figure 7b the dependence of $\Delta H_{\text{apparent}}$ at pH 7.5 on $\Delta H_{\text{ionization}}$. The positive slope from the linear regression to eq 1 indicates that ~0.7 protons are taken up by the TolB-Pal complex. The intercept yields $\Delta H_{\text{binding}}$ corrected for protonation, as −8.8 kcal mol^{-1} and ΔS is +4.4 cal K^{-1} mol^{-1} (average K_d = 27 nM). These data reaffirm that the TolB-Pal interaction is enthalpically and entropically driven at 20 °C but also indicate that an interface side chain becomes protonated during complex formation due to a change in its pK_a. Since protonation does not accompany ColE9 binding to TolB, the location of this ionizable group is most likely within Pal or within a region of TolB that only contacts Pal.

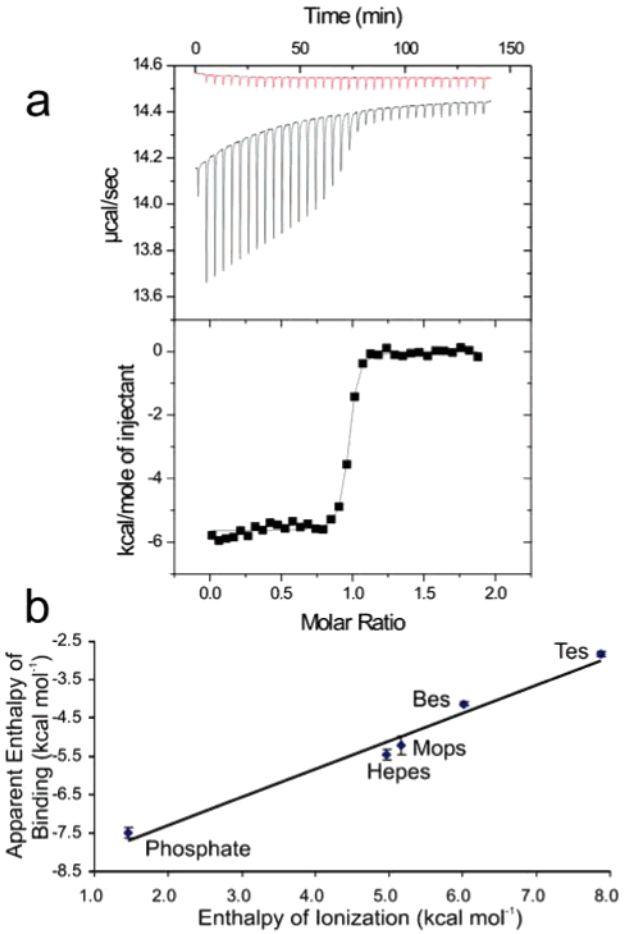

Figure 7. Protonation of a single amino acid accompanies binding of Pal to TolB. (a) ITC binding isotherm at pH 7.5 in 50 mM buffer carried out using a VP-ITC instrument where 281 μM Pal was injected into 31.7 μM TolB. Upper panel shows the raw data, including heats of dilution, and the lower panel shows the data fitted to a single binding site model using a the Origin software supplied by the manufacturer. (b) Apparent enthalpy of binding of Pal to TolB at pH 7.5 as a function of the enthalpy of buffer ionization. Each data point was determined in duplicate (error bars shown). The slope of the linear regression (see eq 1 in text) yields the number of protons taken up by the complex (~0.7), and the y intercept gives the enthalpy of binding corrected for buffer ionization effects (−8.8 kcal mol^{-1}).

Discussion

Functional Implications of the TolB-Pal Complex Structure. While the Tol-Pal system is ubiquitous in Gram-negative bacteria its function has remained elusive. Using GFP-tagged versions of each of the five proteins de Boer and co-workers[44] found recently that the Tol-Pal system co-localizes with the septal ring apparatus, from which they suggest that the function of the complex is to act as an energized tether ensuring appropriate juxtaposition of the outer and inner membranes with respect to the peptidoglycan (PG) layer during cell division. Pal is attached to the OM via a lipoyl group and projects into the periplasm forming noncovalent interactions with the peptidoglycan (PG) cell wall as well as contacting TolB and TolA in the periplasm.[7,8] A recent NMR structure of *H. influenzae* Pal bound to PG precursor (UDP-*N*-acetylmuramyl-L-Ala-α-D-Glu-*m*-Dap-D-Ala-D-Ala) shows that Pal recognizes primarily the *meso*-diaminopimelate moiety of the pentapeptide chain that form the cross-links of the cell wall.[45] A number of Pal residues were identified as interacting with PG, including Phe75, Asp76, Asp110, and Tyr117 (*E. coli* numbering), with Asp110 a potential hydrogen-bond partner for the ϵ-amino group of *m*-Dap and Tyr117 involved in forming hydrophobic contacts with PG. The present structure of the TolB-Pal complex shows that Pal Tyr117 undergoes significant conformational rearrangement and

(43) Velazquez-Campoy, A.; Leavitt, S. A.; Freire, E. *Protein-Protein Interactions: Methods and Protocols*; Fu, H., Ed.; Methods in Molecular Biology 261; Humana Press Inc.: Totowa, NJ, 2004.
(44) Gerding, M. A.; Ogata, Y.; Pecora, N. D.; Niki, H.; de Boer, P. A. J. *Mol. Microbiol.* **2007**, *63*, 1008−1025.
(45) Parsons, L. M.; Lin, F.; Orban, J. *Biochemistry* **2006**, *45*, 2122−2128.

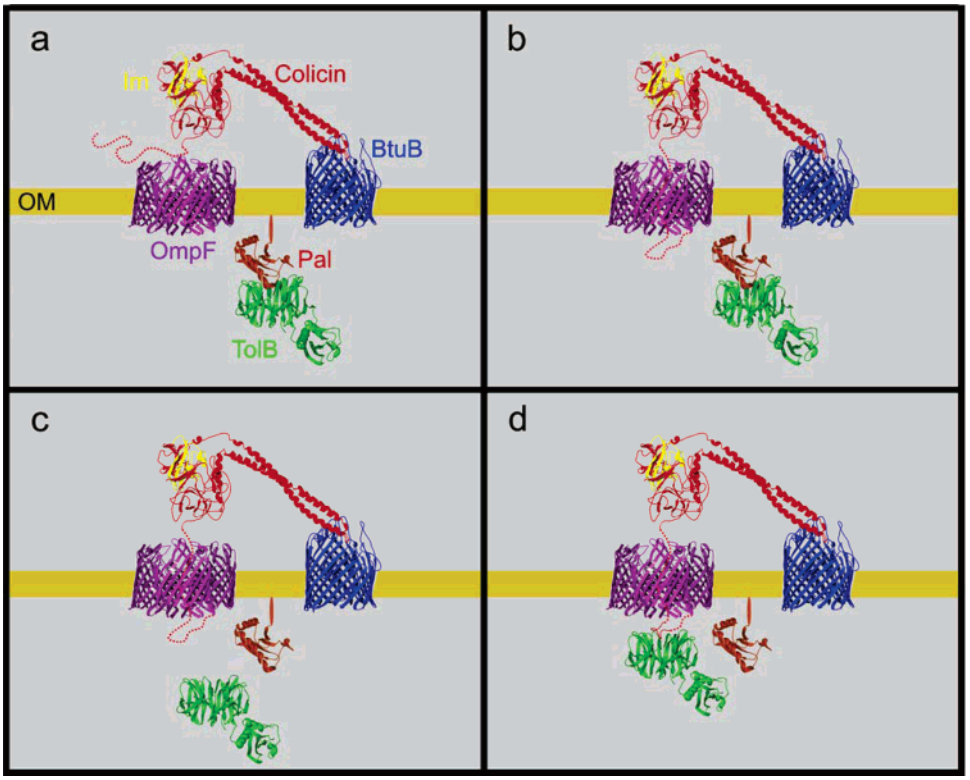

Figure 8. Structural model for the assembly of the colicin translocon at the bacterial cell surface. (a) The figure depicts a model based on five crystal structures: OmpF trimer (PDB, 2OMF), ColE3-Im3 complex (PDB, 1JCH), the complex of the ColE3 R-domain bound to BtuB (PDB, 1UJW), and the most recent structures of TolB in complex with Pal (PDB, 2HQS) and the T-domain NDR of ColE9 (PDB, 2IVZ) both of which bind to the TolB β-propeller. Pal is attached to the OM through a lipoyl group. (a) BtuB-bound colicin recruits OmpF via its natively disordered region. (b) Putative path taken by the NDR to reach the periplasm through the lumen of an OmpF subunit. (c) Competitive recruitment of the TolB-Pal complex. The ColE9 NDR and Pal only have equivalent affinities for TolB when TolB has divalent cations bound within the channel that runs through its β-propeller domain. (d) The ColE9 NDR-TolB complex accomplishes a translocation-competent state, possibly through a locally destabilized OM.

makes important contacts with TolB at Site 1 (Figures 4 and 5). TolB does not coordinate Asp110 directly, but access to this residue becomes restricted in the TolB-Pal complex. On the basis of these structural considerations we conclude that PG and TolB binding to Pal must be mutually exclusive, an observation that is consistent with both in vivo and biochemical data.[8] It follows that Pal associations in the periplasm likely switch from anchoring interactions between the OM and bacterial cell wall to bridging interactions between the OM and IM via the TolQRAB protein complex that traverses the periplasm with this transition driven by the PMF across the inner membrane.

The precise function of TolB is unknown, although it is mostly as an adapter protein coordinating associations between OM/Pal complex with the PG layer and IM. From the present work we can see that Pal binds to one of the most conserved regions of TolB and blocks the central channel running through the β-propeller. Importantly, Pal binding is communicated beyond the immediate vicinity of its binding site to the domain−domain interface, suggesting that Pal may trigger the association/dissociation of other TolB binding partners.

Mechanism of Colicin Entry Across the OM. Disruption of the TolB-Pal complex through gene disruption is known to result in OM instability, leakage of periplasmic contents, and defects in cell division.[11,44,46] In addition, mutants at the TolB-Pal interface have been isolated that cause dissociation of the complex in vivo and in vitro, which also result in OM instability.[10,29,47] Since the TolB-Pal complex is so closely linked to OM stability, this has spawned the idea that colicins may block their association and so cause local instability of the OM, thereby allowing the toxin to translocate to the periplasm. Direct evidence for such a mechanism comes from the work of Bénédetti and co-workers, who secreted N-terminal T-domains of colicins into the periplasm via the general secretory (Sec) apparatus.[46,48,49] This generated *tol*-like phenotypes where cells became 'leaky', resistant to colicins, and showed diminished cross-linking between TolB and Pal in vivo. The question remains however as to how the colicin T-domains are able to recruit TolB from its complex with Pal? This question has now been answered by the two structures of TolB bound to the ColE9 T-domain[29] and Pal (present work). TolB is competitively recruited from its complex with Pal, with the colicin binding at the Pal site and contacting approximately one-half the TolB β-propeller residues contacted by Pal.

Placed in the context of previous structural information we can speculate what the early phases of colicin-receptor assembly at the OM might look like (Figure 8): (i) Enzymatic colicins bind the primary receptor BtuB through their coiled-coil receptor binding domain[25] and recruit OmpF via the NDR,[26] although the precise binding site for this porin has yet to be elucidated;

(46) Henry, T.; Pommier, S.; Journet, L.; Bernadac, A.; Gorvel, J. P.; Lloubès, R. *Res. Microbiol.* **2004**, *155*, 437−446.
(47) Ray, M.-C.; Germon, P.; Vianney, A.; Portalier, R.; Lazzaroni, J. C. *J. Bacteriol.* **2000**, *182*, 821−824.
(48) Bouveret, E.; Rigal, A.; Lazdunski, C.; Bénédetti, H. *Mol. Microbiol.* **1997**, *23*, 909−920.
(49) Bouveret, E.; Journet, L.; Walburger, A.; Cascales, E.; Bénédetti, H.; Lloubès, R. *Biochemie* **2002**, *84*, 413−421.

(ii) The TolB-binding epitope is also present in the colicin NDR, which is thought to reach the periplasm by passing through the lumen of an OmpF pore;[25,28] (iii) The colicin NDR is able to competitively recruit TolB by having the same binding affinity for TolB in its metal-bound state as Pal;[29] (iv) The colicin NDR and TolB associate triggering translocation across the OM, which becomes destabilized as a result TolB-Pal dissociation.

Competitive Recruitment of TolB Reveals a Novel Binding Mechanism for a Natively Disordered Protein. Natively disordered regions of proteins are characterized by contiguous segments of low sequence complexity, having a high proportion of glycine and polar/charged amino acids and relatively few bulky hydrophobic residues.[50,51] Computational analysis has identified NDRs as widespread in biological systems, particularly in eukaryotic proteomes, and highlighted their prevalence in disease states.[52] NDRs, which can be associated with an entire protein or part of protein, tend to be highly mobile with no stable structure and can have one or more linear binding epitopes contained within them. This lack of structure and an extended Stokes radius can lead to 'fly casting',[53] where proteins can 'fish' for binding partners. This is a particularly effective means of recruiting protein assemblies at membrane surfaces. For example, in mammalian endocytosis the NDRs of adapter proteins recruit clathrin at the membrane surface,[54] and in colicin translocation BtuB-bound colicin recruits OmpF at the bacterial cell surface.[26] The unfolded nature of NDRs also allows them to adopt extended conformations when bound to protein partners, as seen in the inhibitory conformations adopted by cyclin-dependent kinase inhibitors[55] and the thrombin inhibitor hirudin.[56] TolB capture by the ColE9 T-domain highlights 'competitive recruitment' as another weapon in the armory of NDRs. This recruitment is achieved through a combination of molecular mimicry and prevention of a conformational change that is induced by the cognate partner Pal. We speculate that competitive recruitment will be observed for other NDRs, although the specific details of such recruitment will likely differ.

One of the remarkable observations from this work is that a 16-residue natively unfolded colicin polypeptide and Pal have similar affinities for TolB ($K_d \approx 90$ nM) even though Pal is 10-times larger and folded. Several factors contribute to this equivalence. First, although Pal buries twice as much accessible surface area as the ColE9 NDR and engages in more than twice as many intermolecular hydrogen bonds, the resulting complex with TolB involves energetically costly conformational changes to both proteins. The colicin NDR does not induce any structural changes in TolB but has to fold into a single, distorted conformation that is stabilized by many intramolecular hydrogen bonds. This disorder−order transition presumably explains why TolB binding by ColE9 is enthalpically favorable but entropically unfavorable. Second, since the colicin is initially unfolded it can be molded to the TolB-binding surface, explaining the greater degree of shape complementarity of its complex with TolB, aided by the burial of two tryptophans, one (Trp46) within a pocket on the TolB surface that is partially occluded in the TolB-Pal complex. Notwithstanding the structural changes in the TolB-Pal complex, binding is both enthalpically and entropically favored, which we speculate is due to expulsion of water from the large protein−protein interface. Binding is also accompanied by protonation of a residue at the TolB-Pal interface, which is not observed in TolB-ColE9 binding. Third, the colicin mimics key interactions that likely comprise the TolB-Pal hotspot. This includes hydrogen bonds involving ColE9 Glu42 and Pal Glu116; mutation of TolB residues involved in both networks (His246, Thr292) obliterates binding to colicin and Pal.[29] Fourth, all of the above account for significant binding of the colicin to TolB but is still an order-of-magnitude weaker affinity than Pal ($K_d \approx 0.9$ μM). This is because electrostatics also play a role in the colicin NDRs' ability to competitively recruit TolB from its complex with Pal. Two divalent cations bound within the TolB β-propeller channel switch the surface electrostatics of the binding site from negative to positive. This improves binding of the negatively charged colicin NDR by >10-fold while only slightly weakening the binding of Pal for TolB, from 27 to 90 nM.[29]

Acknowledgment. This work was supported by The Wellcome Trust and the Biotechnology and Biological Sciences Research Council of the United Kingdom. We acknowledge the ESRF (Grenoble) for provision of synchrotron radiation facilities and Vladimir Levdikov (YSBL), Jennifer Potts (YSBL/York Biology), and the C.K. lab for helpful discussions and comments on the manuscript. We also thank Nick Housden (York) for production of Figure 8.

JA070153N

(50) Fink, A. L. *Curr. Opin. Struct. Biol.* **2005**, *15*, 1−7.
(51) Dyson, H. J.; Wright, P. E. *Nat. Rev. Mol. Cell. Biol.* **2005**, *6*, 197−208.
(52) Ward, J. J.; Sodhi, J. S.; McGuffin, L. J.; Buxton, B. F.; Jones, D. T. *J. Mol. Biol.* **2004**, *337*, 635−645.
(53) Shoemaker, B. A.; Portman, J. J.; Wolynes, P. G. *Proc. Natl. Acad. Sci. U.S.A.* **2000**, *97*, 8868−8873.
(54) Dafforn, T. R.; Smith, C. J. J. *EMBO Rep.* **2004**, *5*, 1046−1052.
(55) Russo, A. A.; Jeffrey, P. D.; Patten, A. K.; Massague, J.; Pavletich, N. P. *Nature* **1996**, *382*, 325−331.
(56) Grutter, M. G.; Priestle, J. P.; Rahuel, J.; Grossenbacher, H.; Bode, W.; Hofsteenge, J.; Stone, S. R. *EMBO J.* **1990**, *9*, 2361−2365.